Tetrahedron 71 (2015) 308–314

Contents lists available at ScienceDirect

Tetrahedron

journal homepage: www.elsevier.com/locate/tet

Lateral extension induces columnar mesomorphism in crucifix shaped quinoxalinophenanthrophenazines

Ala'a O. El-Ballouli [a], Himadri Kayal [b], Chen Shuai [b], Tarek A. Zeidan [a], Farah S. Raad [a], Siwei Leng [c], Brigitte Wex [d], Stephen Z.D. Cheng [c], S. Holger Eichhorn [b,*], Bilal R. Kaafarani [a,*]

[a] Department of Chemistry, American University of Beirut, Beirut 1107-2020, Lebanon
[b] Department of Chemistry and Biochemistry, University of Windsor, Windsor, ON N9B 3P4, Canada
[c] Institute of Polymer Science and Engineering, Department of Polymer Science, The University of Akron, Akron, OH 44325-3909, USA
[d] Department of Natural Sciences, Lebanese American University, Byblos, Lebanon

ARTICLE INFO

Article history:
Received 2 September 2014
Received in revised form 6 November 2014
Accepted 17 November 2014
Available online 21 November 2014

This paper is dedicated to Professor Makhlouf J. Haddadin on the occasion of his 80th birthday and 50 years of outstanding service to the American University of Beirut

ABSTRACT

Reported here is the columnar mesomorphism of board shaped dyes based on quinoxalino[2′,3′:9,10]phenanthro[4,5-*abc*]phenazine (TQPP) derivatives that was induced by an increase in lateral bulk. TQPP derivatives with protons, *tert*-butyl and 4-*tert*-butyl-phenyl groups in positions 2 and 11 are compared, as well as dodecylthio, dodecyloxy, phytanylthio, and phytanyloxy side-chains. Only derivatives with 4-*tert*-butyl-phenyl groups display columnar liquid crystal phases over wide ranges of temperature while all other TQPPs are not liquid crystalline except for the compound with *tert*-butyl groups and phytanyloxy side-chains that shows a Col_r mesophase over a temperature range of 26 °C. The sole attachment of phytanyl groups does not effectively induce columnar mesophases. However, the lateral attachment of bulky groups to the TQPP core induces columnar mesomorphism because of the in-plane aspect ratio decrease and the favored twisted or helical π-stacking of the molecules in columns rather than the parallel co-planar packing.

1. Introduction

Columnar mesophases of aromatic dyes have intrigued researchers' curiosity because of their potential applications as organic semiconductors and dyes in opto-electronic devices. Their self-organization generates unique anisotropic structures with distinctive properties such as self-healing of defects and high charge-carrier mobility and exciton diffusion lengths along the stacking axis.[1–12] Columnar mesophases have been successfully employed as organic semiconductors and absorbers in OPV,[13–17] OFET,[18–25] and OLED[26,27] devices but most of this work has been limited to columnar mesophases of discotic liquid crystals that consist of disc-shaped central cores to which multiple flexible chains are symmetrically attached. Deviation from the conventional disc-shape (low in-plane aspect ratio)[28] and high symmetry has been experimentally[29–33] and computationally[34–39] shown to critically affect, often diminish, columnar mesomorphism. However, the incorporation of donor-acceptor structures for the control of frontier orbital energies as well as absorption and emission properties often dictates less symmetric molecular structures of higher in-plane aspect ratios.[40]

Typical examples with large in-plane aspect ratios are board-shaped polyaromatic dyes, such as quinoxalino[2′,3′:9,10]phenanthro[4,5-*abc*]phenazine (TQPP)-based compounds that usually do not self-organize into columnar mesophases. Lee and co-workers reported the tuning of electronic properties and self-assembly of TQPP-based compounds by changing the R group (Fig. 1).[41] In previous reports, Harris' and our groups showed that sufficiently large and branched side-chains in positions 7, 8, 15, and 16 of the TQPP core induce high temperature mesomorphism,[42,43] but not columnar mesophases typically observed in related but less rigid tetracatenar liquid crystals. Formation of columnar mesophases was observed only for TQPP derivatives that have *tert*-butyl groups as lateral substituents in 2 and 11 positions.[44] This observation prompted us to investigate the effect of lateral substituents in more detail. Reported here is the mesomorphism of TQPP-based compounds **2**–**5** (Fig. 1) with lateral *tert*-butyl and 4-*tert*-butyl-phenyl groups at positions 2 and 11 and dodecylthio and phytanylthio groups attached at carbons 7, 8, 15, and 16. Their mesomorphism is compared to that of the previously reported TQPP

* Corresponding authors. E-mail addresses: eichhorn@uwindsor.ca (S.H. Eichhorn), bilal.kaafarani@aub.edu.lb (B.R. Kaafarani).

http://dx.doi.org/10.1016/j.tet.2014.11.050
0040-4020/

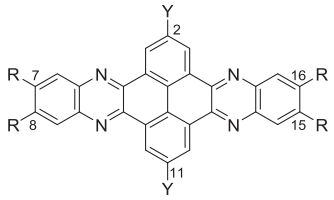

1. Y = H; R = $SC_{12}H_{25}$; **TQPP-[H]$_2$-[SC$_{12}$H$_{25}$]$_4$**
2. Y = *t*-Bu; R = $SC_{12}H_{25}$; **TQPP-[*t*-Bu]$_2$-[SC$_{12}$H$_{25}$]$_4$**
3. Y = *t*-Bu; R = $SC_{20}H_{41}$; **TQPP-[*t*-Bu]$_2$-[SPhytanyl]$_4$**
4. Y = 4-*t*-Bu-Ph; R = $SC_{12}H_{25}$; **TQPP-[*t*-Bu-Ph]$_2$-[SC$_{12}$H$_{25}$]$_4$**
5. Y = 4-*t*-Bu-Ph; R = $SC_{20}H_{41}$; **TQPP-[*t*-Bu-Ph]$_2$-[SPhytanyl]$_4$**
6. Y = *t*-Bu; R = $OC_{12}H_{25}$; **TQPP-[*t*-Bu]$_2$-[OC$_{12}$H$_{25}$]$_4$**
7. Y = *t*-Bu; R = $OC_{20}H_{41}$; **TQPP-[*t*-Bu]$_2$-[OPhytanyl]$_4$**

Fig. 1. Chemical structures of the studied TQPP structures. Compounds **3**–**5** are reported for the first time.

derivatives **1**,[45,46] **6**,[47] and **7**,[44] (Fig. 1) to illustrate the influence of lateral substituents on the formation of columnar mesophases and to compare derivatives with oxygen and thio ether linking groups.

2. Results and discussion

2.1. Synthesis

The synthesis of compounds **1**,[45] **2**,[47] **6**,[47] and **7**[44] has been reported previously. A related approach via the 2,7-disubsituted tetraketopyrenes **11** as key intermediates was chosen for the synthesis of the new compounds **3**–**5** (Scheme 1). Compound **11** was prepared by the catalytic oxidation of 2,7-disubstituted pyrene **10** using ruthenium(III) chloride and sodium(*meta*)periodate.[48] Phytanylthiol (**9**) was prepared by the reduction of phytol to phytanol, which upon reaction with HBr and H_2SO_4 lead to phytanyl bromide. Refluxing phytanyl bromide with thiourea in ethanol and NaOH afforded **9**[49] with an overall yield of 45% over the three steps. 2,7-Di-*tert*-butylpyrene was prepared by the reaction of pyrene and *tert*-butylchloride in the presence of $AlCl_3$. The synthesis and X-ray structure of **10b** are reported elsewhere.[50] Briefly, 2,7-dibromopyrene[51–53,50] (**10a**) was synthesized by the reduction of pyrene into tetrahydropyrene, which upon electrophilic aromatic substitution in the presence of bromine and subsequent oxidation in the presence of bromine and carbon disulfide, lead to **10a**. The Suzuki coupling of 2,7-dibromopyrene **10a** with 4-*tert*-butyl-phenylboronic acid afforded **10b**.[50] The condensation of **11** with 1,2-dichloro-4,5-phenylenediamine **12** (commercially available) yielded **13**, which upon reaction with the corresponding alkylthiol furnished compounds **2**–**5**. Substitution of all four chlorine atoms with dodecylthiol is high yielding but substitution with the branched phytanylthiol gives significantly lower yields, probably due to steric hindrance.

2.2. Mesomorphism

Scheme 2 summarizes the thermal phase behavior of compounds **1**–**7** based on polarized optical microscopy (POM), differential scanning calorimetry (DSC), thermal gravimetric analysis (TGA) and variable temperature X-ray diffraction (vt-XRD) investigations.

Thermal stability of the new compounds **2**–**5** was probed by thermal gravimetric analysis (TGA) under He at a heating rate of 2 °C/min. Decomposition temperatures are given as the temperature at which 0.1% wt loss has occurred because these values agree with the long term thermal stability observed by POM and NMR measurements of heated compounds. Values based on the extrapolated onset of weight loss are 30–50 °C higher. Thermally most stable are compounds **2** (270 °C) and **4** (274 °C) with dodecyl chains while compounds **3** (246 °C) and **5** (254 °C) with phytanyl chains are slightly less stable. In contrast, the exchange of *tert*-butyl groups by 4-*tert*-butyl phenyl groups does not significantly affect

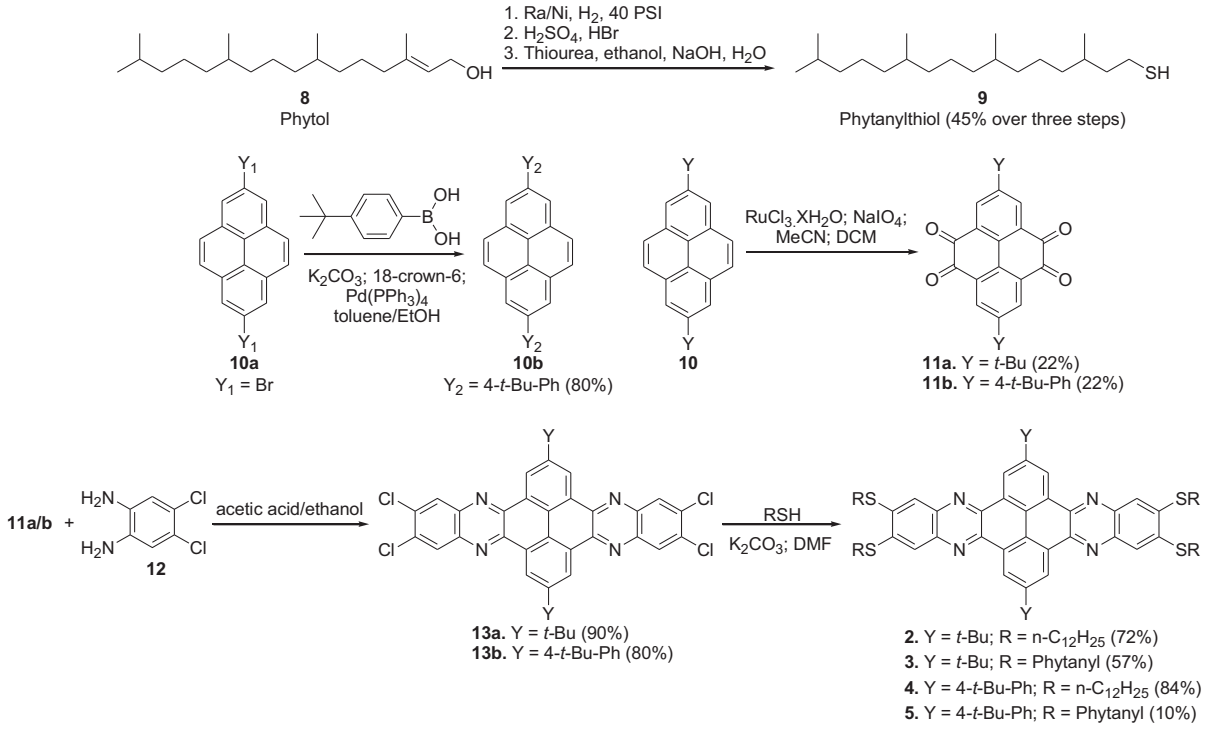

Scheme 1. Synthetic Scheme of compounds **2**–**5**.

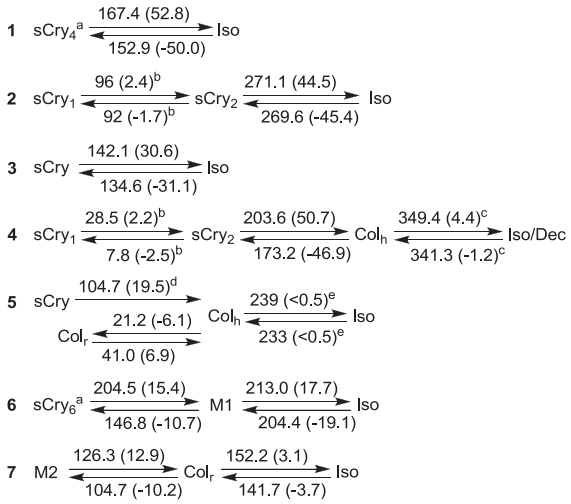

Scheme 2. Thermal phase behavior of compounds **1**–**7** based on POM, DSC, and XRD. Transition temperatures and enthalpies based on DSC (10 °C/min) are given in °C and kJ mol^{-1}, respectively. Phase assignment: (s)Cry=(soft) crystal, Col$_h$=hexagonal columnar mesophase, Col$_r$=rectangular columnar mesophase, Iso=isotropic liquid, Dec=decomposition, M=unknown mesophase. [a]Several crystal to crystal transitions occur (see Supplementary data for details). [b]Peak temperature of a broad transition; [c]Transition occurs above the on-set of thermal decomposition; [d]Observed only in the 1st-heating run; [e]Determined by POM and not observed by DSC.

thermal stability. This may be expected as the phenyl rings are not in conjugation with the TQPP core based on the similarity of the absorption spectra of **3** and **5** above 350 nm in solution and as thin films (Fig. 2 and Table S3).

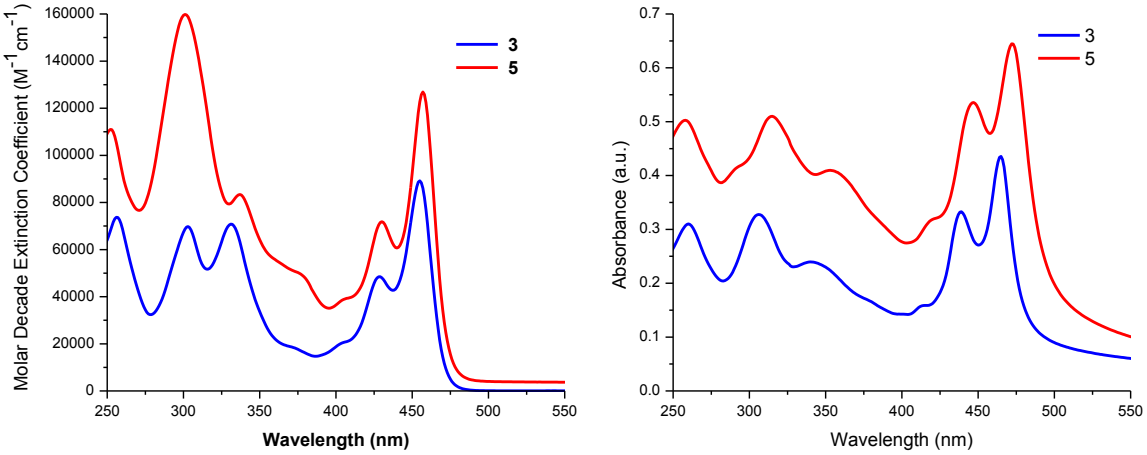

Fig. 2. Absorption spectra of TQPPs **3** and **5** in solution (left, DCM) and as thin films on quartz (right).

TQPP derivatives **1** to **3** display crystal phases that melt into isotropic liquids at or below the onsets of their thermal decomposition. Their crystal phases, however, are best categorized as soft crystal (meso)phases because the crystallites easily deform under pressure similar to a fluid of high viscosity.[54] X-ray diffraction patterns (see Supplementary data) and the high enthalpies of the melting transitions are in agreement with the assigned phases and phase transitions in Scheme 2. Attachment of phytanyl side-chains with multiple branching points in TQPP **3** lowered the melting point by 130 °C in comparison to TQPP **2** but did not fully suppress crystallization and neither induced a liquid crystal phase.

Diffraction patterns of the three solid phases of compounds **1** to **3** show a larger number of reflections in the small and wide-angle ranges, which is consistent with 3-dimensionally ordered soft crystal phases rather than 2-dimensionally ordered liquid crystal phases. However, the sCry phase of TQPP **3** shows significantly fewer and broader reflections than the sCry phases of TQPPs **1** and **2** due to the more amorphous packing of the branched phytanyl side-chains. The structures of the sCry phases of **1** and **2** cannot be easily deduced from the 1-dimensional XRD patterns while compound **3** most likely arranges in a layered structure. Reflections up to the 4th order can be assigned if the smallest angle reflection of **3** is assigned as the principle reflection of the layer spacing. However, the calculated d-spacing of 32.6 Å is 38% smaller than the length of the extended molecule (Table 1). This difference is unlikely caused solely by interdigitation and softening of the phytanyl side-chains. More likely is a tilted orientation of the TQPP core with regard to the layer normal. Diffraction studies on single crystals of TQPP **1** and related crystalline TQPP derivatives have confirmed layer structures for several of these compounds.[44]

The complete absence of liquid crystal phases for compounds **2** and **3** is surprising as their oxygen ether analogs **6** and **7** display short range liquid crystal phases.[44] Exchange of oxygen ethers by thioethers often enhances mesomorphism because of the larger polarizability of sulfur although most experimental results for discotic liquid crystals reveal only minimal changes to their mesomorphism (e.g., hexaalkylthio/oxy triphenylenes and octaalkylthio/oxy phthalocyanines).[28] The absence of liquid crystal phases for thioether compounds **2** and **3** is caused by an increase in melting temperatures when compared to their oxygen ether analogs **6** and **7**. In fact, TQPP **2** melts 58 °C above the isotropization (clearing) temperature of **6** and TQPP **3** melts just 10 °C below the isotropization temperature of **7** (Scheme 2).

Attachment of lateral *tert*-butylphenyl groups in TQPPs **4** and **5** induces columnar liquid crystal phases that are stable over wide ranges of temperature (>100 °C) as confirmed by POM, DSC, and XRD (Scheme 2). TQPP **4** melts into a hexagonal columnar mesophase at 200 °C and clears at 350 °C, 75 °C above its onset of thermal decomposition. Both, dendritic fan-shaped defect textures with pseudo-isotropic areas of homeotropic domains and the diffraction patterns containing an intense (10) reflection and weak (11) and (20) reflections of relative lattice spacings 1:√3:2 confirm the hexagonal symmetry of the plane group of the columnar mesophase (Fig. S16 and Table S1 in the Supplementary data). The broadness of the (10) reflection indicates a rather disordered packing of the columns that is likely caused by the elliptical shape of the molecules. Less affected by the elliptical shape is the intracolumnar packing order as indicated by the intense broad reflection at 0.35 nm (3.5 Å).

A lattice parameter of 2.93 nm was calculated for the hexagonal plane lattice of TQPP **4** at 538 K (265 °C), which gives an area per molecule S_{hex} of 7.43 nm^2 ($S_{hex}=a^2\times\sqrt{3}/2$) and a volume per

Table 1
Estimated and measured molecular dimensions for TQPPs **1**–**7**

Comp.	L_{max} (nm)	W_{max} (nm)	A.R.	S_{max} (nm^2)	V_{max} (nm^3)	V_{liq} (nm^3)	S_{XRD} (nm^2)	V_{XRD} (nm^3)
1	4.7	0.9	5.2	4.23	1.48	2.23	n.a.	1.73[b]
2	4.7	1.1	4.3	5.17	1.81	2.38	n.a.	n.a.
3	5.2	1.1	4.7	5.72	2.00	3.18	n.a.	n.a.
4	4.8	2.0	2.4	9.60	3.36	2.53	7.43	2.60
5	5.2	2.0	2.6	10.40	3.64	3.32	9.10	3.11
6	4.7	1.1	4.3	5.17	1.81	s. t. **2**[a]	n.a.	n.a.
7	5.2	1.1	4.7	5.72	2.00	s. t. **3**[a]	n.a.	n.a.

L_{max}=maximum length of molecule with extended side-chains. W_{max}=maximum width of the aromatic core. A.R.=maximum aspect ratio in the plane of the aromatic core calculated as L_{max}/W_{max}. S_{max}=maximum area of molecule calculated as $L_{max}\times W_{max}$. $V_{max}=S_{max}\times 0.35$=maximum volume per molecule based on a stacking distance of 0.35 nm. V_{liq} is the more realistic volume per molecule in the liquid phase calculated as the sum of volumes of the core and aliphatic side-chains as described in the Supplementary data. Core volumes are estimated from single crystal data and experimental volume increments and the volumes of aliphatic side chains in their liquid phases at a given temperature are calculated based on empirical equations derived from dilatometric measurements.[55] Values for TQPPs **1**, **2** and **4** were calculated for a temperature of 265 °C and values for TQPPs **3** and **5** for a temperature of 120 °C to allow comparison with the values obtained from the XRD data of the Col_h mesophases of TQPPs **4** and **5**. S_{XRD} and V_{XRD} are the molecular cross-sections and volumes in the hexagonal columnar mesophases determined by XRD based on one molecule per columnar slice.

[a] s. t.=similar to.

[b] This value is based on the unit cell dimensions of the high temperature monoclinic crystal phase.[44]

molecule of 2.60 nm^3 for a stacking distance of 0.35 nm. Area and volume per molecule determined by XRD are in good agreement with the estimated values listed in Table 1. We conclude from the observed dimensions and the stacking model shown in Fig. 3 that the long axes of the cores of TQPP **4** (and **5**) must be at an angle to accommodate the steric bulk of the out-of-plane *tert*-butylphenyl groups. This type of arrangement also distributes the aliphatic side-chains more evenly around the columnar stacks, which is essential for the formation of a hexagonal columnar mesophase. The most probable columnar structure is a helical arrangement of the molecules that has been confirmed for similar compounds.[56,57] However, diffraction data of unaligned samples of TQPP **4** (and **5**) do not provide any evidence for a helical structure and no attempt was made to study aligned monodomains of TQPPs **4** and **5**. Consequently, we cannot exclude other possible stacking structures with ordered or disordered rotations of the stacking molecules with regard to each other.

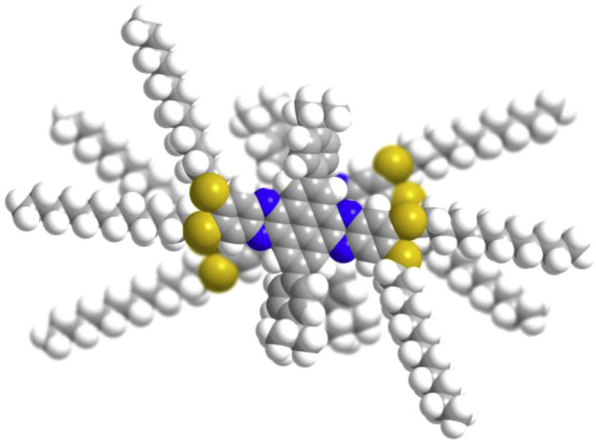

Fig. 3. Cartoon illustrating the proposed helical arrangement in the Col_h mesophases of TQPPs **4** and **5**.

TQPP **5** forms a soft crystal phase when precipitated from solution. The soft crystal phase irreversibly melts into a hexagonal columnar liquid crystal phase at 105 °C, which clears into an isotropic liquid at 240 °C. No soft crystal phase is formed on cooling but, instead, the compound displays a rectangular columnar mesophase below 21 °C. Again, the phase assignment is confirmed by characteristic defect textures (Fig. 4) and diffraction patterns (Fig. 5).

Diffraction patterns at 120 °C (Fig. 5) and 200 °C (Fig. S18) both show small angle reflections (10), (11), and (20) with a ratio of 1:√3:2. These patterns and the observation of pseudo isotropic areas of homeotropic domains (Fig. 4) confirm the presence of a Col_h phase at the given temperatures. The (10) reflection is broadening with decreasing temperature and the (11) and (20) reflections eventually disappear at 40 °C (Fig. S18). This change is interpreted as a gradual increase in distortion of the hexagonal packing that eventually leads to the formation of the Col_r below 21 °C (Fig. 5). However, the wider range of temperature of the Col_h phase and the lesser broadening of the (10) reflection compared to TQPP **4** confirms a much better compatibility of TQPP **5** with a hexagonal columnar arrangement. Noteworthy is the short stacking distance of 0.342 nm at 120 °C that increases to 0.347 nm at 200 °C and in the Col_r mesophase. However, the persistence length of the stacking increases with decreasing temperature and is the highest in the Col_r mesophase as indicated by the increase in intensity and narrowing of the wide angle (001) reflection.

Estimated molecular dimensions of TQPP **5** agree well with observed dimensions of the columnar mesophases (Table 1). A columnar cross section of 9.10 nm^2 and a volume of 3.11 nm^3 per columnar stacking unit are calculated based on a lattice parameter of a=3.24 nm and a stacking distance of 0.342 nm for the Col_h phase at 120 °C. Both cross section and volume decrease with temperature and the smallest values are obtained in the Col_r mesophases. A projected area per molecule of 8.36 nm^2 (molecules are tilted with regard to the stacking axis) and a volume per molecule of 2.90 nm^3 are calculated based on lattice parameters of a=7.25 nm and b=2.30 nm, a stacking distance of 3.47 Å and the occupancy of 2 molecules per unit plane and cell. A reduction in the volume per molecule is expected for a transition from a Col_h to a higher ordered Col_r mesophase.[58] All (hk) reflections obtained for the Col_r mesophase satisfy the condition $h+k=2n$ and, consequently, the diffraction data are not sufficient for a distinction between the centered c2mm and the p2gg lattices.

A comparison of TQPPs **1**, **2**, and **4** shows how the lateral extension from hydrogen (TQPP **1**) to *tert*-butyl (TQPP **2**) to 4-*tert*-butylphenyl (TQPP **4**) first stabilizes the crystalline phase (TQPPs **1** and **2**) but finally induces columnar mesomorphism in TQPP **4**. This, perhaps surprising, can be rationalized with differences in intermolecular interactions and a reduction of the aspect ratios in the order **1**>**2**>**4**. TQPP **1** has an aspect ratio of 4.7 and packs into layered crystalline structures but does not form liquid crystal phases. Instead, it melts into an isotropic liquid at a comparatively low temperature of 167.4 °C. Introduction of *tert*-butyl groups at the 2 and 11 positions of **2** decreases the aspect ratio to 4.3 and interferes with the formation of layered structures with parallel close co-facial packing of the molecules. Close co-facial packing of the aromatic cores is possible only if the long-axes of the molecules are rotated with regard to each other to generate a helical-type

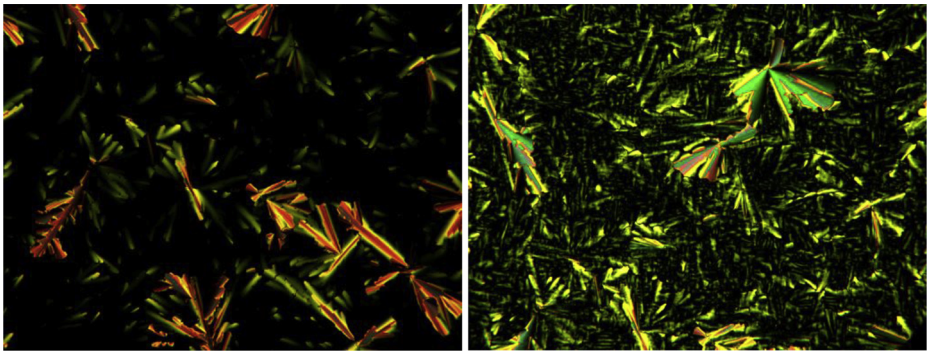

Fig. 4. POM micrographs of the Col_h (left) and Col_r (right) phases of TQPP **5** between glass slides at 215 °C and 17 °C on cooling from the isotropic liquid at 2 °C/min (crossed polarizers, 200× magnification). Dark areas around the dentritic texture are homeotropically (vertically) aligned domains.

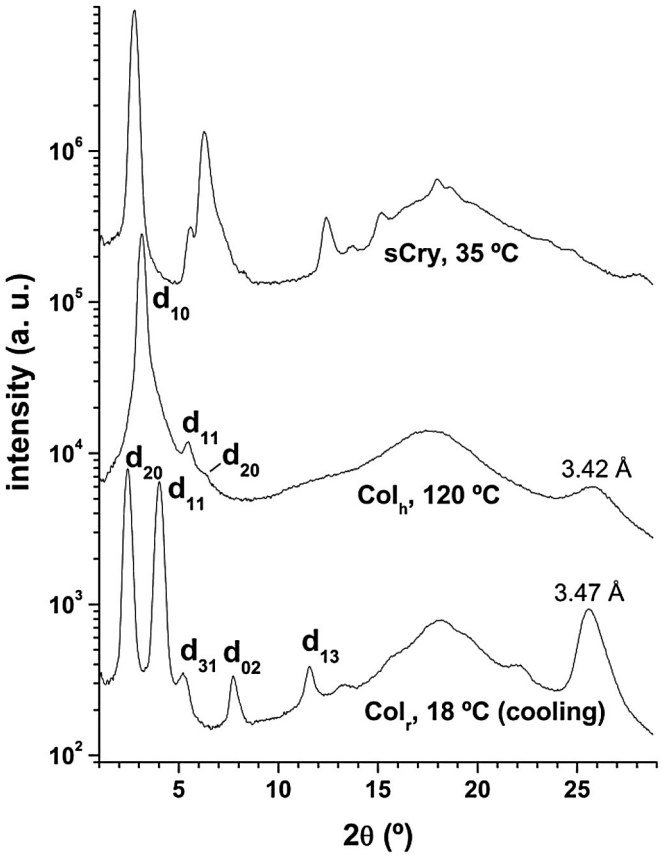

Fig. 5. Diffraction patterns of TQPP **5** at 35 °C (as precipitated; soft crystal phase), at 120 °C (Col_h), and after cooling from 150 °C to 18 °C (Col_r).

columnar stack or the molecules arrange in slipped stacks as observed for some laterally substituted polyacenes.[59] However, TQPP **2** does not display a liquid crystal phase mainly because its soft crystal phase persists up to 271 °C. Attachment of 4-*tert*-butylphenyl groups in TQPP **4** significantly reduces the aspect ratio to 2.4 and promotes columnar stacking because the out-of-plane phenyl groups sterically disfavor parallel co-facial packing. In fact, the high clearing temperature of 349 °C of the Col_h mesophase of TQPP **4** is evidence for a stabilization of the columnar mesophases that is likely caused by a helical stacking of the molecules. Induction of helical stacking by phenyl groups attached to the aromatic core has been reported for other discotic liquid crystals.[57]

Exchange of the linear dodecyl chains by branched phytanyl chains drastically reduces transition temperatures and broadens the temperature range of the columnar mesophases of TQPP **5** in comparison to TQPP **4**, but does not induce mesomorphism in TQPP **3**. Clearly, the combination of lateral extension with 4-*tert*-butylphenyl groups and the increase in packing volume of the side-chains by the attachment of phytanyl chains is crucial for the enhancement of columnar mesomorphism in TQPP **5**. A room temperature columnar mesophase is obtained because crystallization from the mesophase is suppressed by the branched chains and the presence of many isomers. In fact, TQPP **5** is not a single compound because each of the 4 phytanyl chains contains 3 racemic chiral carbons that generate 4096 diastereomers and enantiomers. Other advantages are the sufficiently low clearing temperature that generates a thermally stable isotropic liquid phase as well as a more fluid Col_h phase that spontaneously aligns homeotropically between glass substrates. Both properties are advantages for the processing of these materials. We also note that the stacking order in the hexagonal and, in particular, rectangular columnar mesophases remains high despite the incorporation of multiple branched side-chains.

3. Conclusions

The board-shaped TQPP core is transformed into a potent columnar mesogen TQPP **5** by the lateral attachment of 4-*tert*-butylphenyl groups at carbons 2 and 11 and the use of multiple branched phytanyl side-chains. Lateral extension of the core to crucifix shaped structures is essential for the formation of hexagonal columnar mesophases while the incorporation of phytanyl side-chains is most effective in the control of phase transition temperatures. Surprisingly, TQPPs with oxygen ether linking groups show a higher propensity for mesomorphism than their thio ether analogs.

4. Experimental

4.1. General synthesis

1-Dodecanethiol ($C_{12}H_{25}SH$) is commercially available. Phytanylthiol (**9**),[49] 2,7-dibromopyrene (**10a**),[52,53] 2,7-di-*tert*-butylpyrene-4,5,9,10-tetraone (**11a**),[48] and 2,7-bis-(4-*tert*-butylphenyl) pyrene (**10b**)[50] were prepared according to literature procedures. Syntheses of **1**,[45] **2**,[47] **6**,[47] and **7**[44] were previously reported.

*4.1.1. TQPP-[t-Bu]$_2$-[Cl]$_4$ (**13a**).* 2,7-Di-*tert*-butyltetraketopyrene (**11a**) (1.00 g, 2.67 mmol) was added to a solution of 4,5-dichloro-1,2-phenylenediamine (1.00 g, 0.01 mol) in ethanol:acetic acid (1:1). The solution was refluxed for 24 h. The mixture was cooled, filtered and the solid was triturated using hot toluene via soxhlet extraction to obtain **13a** as dark yellow solid (1.40 g, 80%), mp >300 °C. The solid was used for the next step without further

purification. HRMS-MALDI (m/z): $[M+H]^+$ Calcd for $C_{36}H_{27}N_4Cl_4$, 655.09; Found, 655.08.

*4.1.2. TQPP-[t-Bu]$_2$-[Sphytanyl]$_4$ (**3**).* The title compound was synthesized according to a modified literature procedure.[60] TQPP-[*t*-Bu]$_2$-[Cl]$_4$ (**13a**) (1.3 g, 1.98 mmol) and K_2CO_3 (15.1 g, 0.11 mol) was suspended in dry DMF and purged with argon for one hour. Distilled phytanylthiol (**9**) (9.35 g, 29.7 mmol) was transferred to the reaction mixture through a syringe. The mixture was heated at 80 °C for one week. The reaction mixture was cooled down, poured onto water and neutralized with conc. HCl to pH=5. The yellow solid was filtered and washed with water. The product was purified by gradient column chromatography starting from hexanes:-chloroform 9:1 till 7:3 and the solvent was evaporated. The collected solid was recrystalized from heptane/ethanol to obtain **3** as sticky yellow solid (2.00 g, 57%), mp (determined by DSC) 142.1 °C. ^{1}H NMR (300 MHz, $CDCl_3$): δ 9.74 (s, 4H), 8.10 (s, 4H), 3.34–3.27 (m, 8H), 1.92–1.82 (m, 4H), 1.76–1.74 (m, 8H), 1.75 (s, 18H), 1.40–1.18 (m, 84H), 0.98–0.97 (m, 60H). ^{13}C NMR (75.5 MHz, $CDCl_3$): δ 150.68, 142.19, 141.39, 140.67, 129.40, 125.38, 124.01, 123.90, 39.34, 37.50, 37.44, 37.39, 37.27, 37.12, 35.91, 35.19, 35.12, 32.82, 32.78, 32.56, 31.91, 31.23, 27.97, 24.80, 24.49, 24.43, 22.73, 22.63, 19.80, 19.74. Anal. Cald. for $C_{116}H_{190}N_4S_4$: C, 78.76; H, 10.83; N, 3.17; S, 7.25. Found: C, 78.54; H, 10.87; N, 3.15; S, 7.13.

*4.1.3. 2,7-Bis(4-tert-butylphenyl)-4,5,9,10-tetraketopyrene (**11b**).* The title compound was prepared according to a modified literature procedure.[48] 2,7-Bis(4-*tert*-butylphenyl)pyrene (**10b**) (800 mg, 1.71 mmol) was dissolved together with sodium(*meta*)periodate $NaIO_4$ (2.96 g, 0.01 mol) in 50 mL (1:1; CH_2Cl_2:CH_3CN). Ruthenium(III) chloride $RuCl_3 \cdot xH_2O$ (0.09 g, 0.43 mmol) was added along with 32 mL distilled water. The reaction mixture was stirred for 2 days at 40 °C. The brown mixture was poured over H_2O (200 mL) and was extracted using CH_2Cl_2. The organic layer was dried over $MgSO_4$ after which it was evaporated under reduced pressure. The collected solid was then purified using gradient column chromatography 7:3 (hexanes:chloroform) till 100% chloroform as an eluent, the solvent was then evaporated. The title compound **11b** was collected as red solid (200 mg, 22%), mp >300 °C. ^{1}H NMR (300 MHz, $CDCl_3$): δ 8.71 (s, 4H), 7.71 (d, J=8.4 Hz, 4H), 7.57 (d, J=8.4 Hz, 4H), 1.39 (s, 18H). ^{13}C NMR (75.5 MHz, $CDCl_3$): δ 178.13, 153.06, 143.65, 134.46, 133.91, 132.79, 131.25, 126.54, 126.38, 34.81, 31.24.

*4.1.4. TQPP-[4-t-Bu-phenyl]$_2$-[Cl]$_4$ (**13b**).* 2,7-Di-4-*tert*-butylph enyltetraketopyrene (**11b**) (0.10 g, 0.20 mmol) was added to a solution of 4,5-dichloro-1,2-phenylenediamine (0.10 g, 0.56 mmol) in ethanol:acetic acid (1:1). The solution was refluxed for 24 h. The mixture was cooled down, filtered and the solid was triturated using hot toluene via soxhlet extraction to obtain **13b** as dark yellow solid (0.12 g, 80%), mp >300 °C. The solid was used for the next step without further purification. MALDI-TOF (m/z): $[M+H]^+$ Calcd for $C_{48}H_{35}N_4Cl_4$, 809.62; Found, 809.30.

*4.1.5. TQPP-[4-t-Bu-phenyl]$_2$-[SC$_{12}$H$_{25}$]$_4$ (**4**).* The titled compound was synthesized according to a modified literature procedure.[60] TQPP-[4-*t*-Bu-phenyl]$_2$-[Cl]$_4$ (**13b**) (0.23 g, 0.28 mmol) and K_2CO_3 (1.96 g, 14.2 mmol) suspended in dry DMF. A stream of argon gas was passed through the mixture for 1 h. $C_{12}H_{25}SH$ (0.92 g, 4.54 mol) was added. The mixture was heated at 80 °C in oil bath for one week. The reaction mixture was cooled down, poured onto water and neutralized by conc. HCl to pH=5. The yellow solid was filtered and washed with water. The product was purified by gradient column chromatography starting from hexanes:chloroform 9:1 till 6:4 and the solvent was evaporated. The collected solid was recrystallized from heptane to obtain **4** as yellow solid (350 mg, 84%), mp (determined by DSC) 200.6 °C. ^{1}H NMR (300 MHz, $CDCl_3$): δ 9.24 (s, 4H), 7.94 (d, J=8.1 Hz, 4H), 7.64 (d, J=8.1 Hz, 4H), 7.62 (s, 4H), 3.21–3.16 (m, 8H), 1.97–1.88 (m, 8H), 1.65–1.62 (m, 8H), 1.60 (s, 18H), 1.46–1.28 (m, 64H), 0.9–0.85 (t, J=6 Hz, 12H). ^{13}C NMR (75.5 MHz, $CDCl_3$): δ 159.73, 150.28, 140.90, 140.22, 139.15, 138.14, 129.07, 127.70, 125.66, 124.82, 124.52, 122.84, 34.70, 33.25, 31.96, 31.62, 29.80, 29.74, 29.72, 29.51, 29.42, 28.16, 22.72, 14.15. Anal. Cald. for $C_{96}H_{134}N_4S_4$: C, 78.31; H, 9.17; N, 3.81; S, 8.71. Found: C, 78.43; H, 9.14; N, 3.85; S, 8.75.

*4.1.6. TQPP-[p-t-Bu-phenyl]$_2$-[Sphytanyl]$_4$ (**5**).* The titled compound was synthesized according to a modified literature procedure.[60] TQPP-[*p*-*t*-Bu-phenyl]$_2$-[Cl]$_4$ (**13b**) (0.30 g, 0.37 mmol) and K_2CO_3 (2.56 g, 18.6 mmol) suspended in dry DMF. A stream of argon gas was passed through the mixture for 1 h. Distilled phytanylthiol (**8**) (1.13 g, 3.59 mol) was added. The mixture was heated at 80 °C in oil bath for one week. The reaction mixture was cooled down, poured onto water and neutralized by conc. HCl to pH=5. The yellow solid was filtered and washed with water. The product was purified by gradient column chromatography starting from hexanes:chloroform 9:1 till 6:4 and the solvent was evaporated. The collected solid was recrystallized from heptane/ethanol to obtain **5** as sticky yellow solid (70 mg, 10%), mp (determined by POM) 239 °C. ^{1}H NMR (300 MHz, $CDCl_3$): δ 9.44 (s, 4H), 7.99 (d, J=7.5 Hz, 4H), 7.76 (s, 4H), 7.66 (d, J=7.5 Hz, 4H), 3.23–3.20 (m, 8H), 1.96–1.93 (m, 4H), 1.77–1.70 (m, 8H), 1.58 (s, 18H), 1.45–1.10 (m, 84H), 0.97–0.95 (m, 60H). ^{13}C NMR (75.5 MHz, $CDCl_3$): δ 150.52, 141.31, 141.25, 140.48, 139.62, 138.18, 129.45, 127.72, 125.78, 125.21, 124.84, 123.22, 39.36, 37.44, 37.40, 37.34, 37.29, 35.17, 34.72, 32.90, 32.80, 32.73, 31.60, 31.25, 29.71, 27.97, 24.81, 24.54, 22.72, 22.63, 19.74, 19.67, 19.58. $C_{128}H_{198}N_4S_4$: C, 80.02; H, 10.39; N, 2.92; S, 6.68. Found: C, 79.86; H, 10.40; N, 3.05; S, 6.56.

Acknowledgements

This work has been supported by the ACS-PRF (Grant No. 47343-B10), the University Research Board of the American University of Beirut, the Natural Sciences and Engineering Research Council of Canada (NSERC) grant (P\RGPIN-2014-05706), the Canada Foundation for Innovation (CFI), and the Ontario Innovation Trust (OIT). The authors are grateful for this support. B. R. K. and B. W. thank the Arab Fund Scholarship Program for financial support.

Supplementary data

^{1}H NMR, ^{13}C NMR, MALDI-TOF, TGA, DSC, Powder XRD, Calculations of dimensions, and UV of thins films are available in ESI. Supplementary data related to this article can be found at http://dx.doi.org/10.1016/j.tet.2014.11.050.

References and notes

1. Boden, N.; Bushby, R. J.; Clements, J.; Movaghar, B. *J. Mater. Chem.* **1999**, *9*, 2081–2086.
2. Pisula, W.; Zorn, M.; Chang, J. Y.; Müllen, K.; Zentel, R. *Macromol. Rapid Commun.* **2009**, *30*, 1179–1202.
3. Kato, T.; Mizoshita, N.; Kishimoto, K. *Angew. Chem., Int. Ed.* **2006**, *45*, 38–68.
4. Kumar, S. *Chem. Soc. Rev.* **2006**, *35*, 83–109.
5. Laschat, S.; Baro, A.; Steinke, N.; Giesselmann, F.; Haegele, C.; Scalia, G.; Judele, R.; Kapatsina, E.; Sauer, S.; Schreivogel, A.; Tosoni, M. *Angew. Chem., Int. Ed.* **2007**, *46*, 4832–4887.
6. Sergeyev, S.; Pisula, W.; Geerts, Y. H. *Chem. Soc. Rev.* **2007**, *36*, 1902–1929.
7. Kaafarani, B. R. *Chem. Mater.* **2011**, *23*, 378–396.
8. *Self-organized Organic Semiconductors: From Materials to Device Applications*; Li, Q., Ed.; John Wiley & Sons: Hoboken, NJ, 2011.
9. *Liquid Crystals beyond Displays: Chemistry, Physics, and Applications*; Li, Q., Ed.; John Wiley & Sons: Hoboken, NJ, 2012.
10. Sun, Q.; Dai, L.; Zhou, X.; Li, L.; Li, Q. *Appl. Phys. Lett.* **2007**, *91*, 253505/1–253505/3.

11. Zhou, X.; Kang, S.-W.; Kumar, S.; Kulkarni, R. R.; Cheng, S. Z. D.; Li, Q. *Chem. Mater.* **2008**, *20*, 3551–3553.
12. Zhou, X.; Kang, S.-W.; Kumar, S.; Li, Q. *Liq. Cryst.* **2009**, *36*, 269–274.
13. Schmidt-Mende, L.; Fechtenkötter, A.; Müllen, K.; Moons, E.; Friend, R. H.; MacKenzie, J. D. *Science* **2001**, *293*, 1119–1122.
14. Li, L.; Kang, S.-W.; Harden, J.; Sun, Q.; Zhou, X.; Dai, L.; Jakli, A.; Kumar, S.; Li, Q. *Liq. Cryst.* **2008**, *35*, 233–239.
15. Jung, J.; Rybak, A.; Slazak, A.; Bialecki, S.; Miskiewicz, P.; Glowacki, I.; Ulanski, J.; Rosselli, S.; Yasuda, A.; Nelles, G.; Tomovic, Z.; Watson, M. D.; Müllen, K. *Synth. Met.* **2005**, *155*, 150–156.
16. Schmidtke, J. P.; Friend, R. H.; Kastler, M.; Müllen, K. *J. Chem. Phys.* **2006**, *124*, 174704/1–174704/6.
17. Oukachmih, M.; Destruel, P.; Seguy, I.; Ablart, G.; Jolinat, P.; Archambeau, S.; Mabiala, M.; Fouet, S.; Bock, H. *Sol. Energy Mater. Sol. Cells* **2005**, *85*, 535–543.
18. Pisula, W.; Menon, A.; Stepputat, M.; Lieberwirth, I.; Kolb, U.; Tracz, A.; Sirringhaus, H.; Pakula, T.; Müllen, K. *Adv. Mater.* **2005**, *17*, 684–689.
19. Shklyarevskiy, I. O.; Jonkheijm, P.; Stutzmann, N.; Wasserberg, D.; Wondergem, H. J.; Christianen, P. C. M.; Schenning, A. P. H. J.; De Leeuw, D. M.; Tomovic, Z.; Wu, J.; Müllen, K.; Maan, J. C. *J. Am. Chem. Soc.* **2005**, *127*, 16233–16237.
20. Tsao, H. N.; Pisula, W.; Liu, Z.; Osikowicz, W.; Salaneck, W. R.; Müllen, K. *Adv. Mater.* **2008**, *20*, 2715–2719.
21. Chesterfield, R. J.; McKeen, J. C.; Newman, C. R.; Ewbank, P. C.; Da Silva Filho, D. A.; Brédas, J.-L.; Miller, L. L.; Mann, K. R.; Frisbie, C. D. *J. Phys. Chem. B* **2004**, *108*, 19281–19292.
22. Dong, S.; Tian, H.; Song, D.; Yang, Z.; Yan, D.; Geng, Y.; Wang, F. *Chem. Commun.* **2009**, 3086–3088.
23. Hoang, M. H.; Cho, M. J.; Kim, K. H.; Cho, M. Y.; Joo, J.-s.; Choi, D. H. *Thin Solid Films* **2009**, *518*, 501–506.
24. Guo, X.; Xiao, S.; Myers, M.; Miao, Q.; Steigerwald, M. L.; Nuckolls, C. *Proc. Natl. Acad. Sci. U.S.A.* **2009**, *106*, 691–696.
25. Hoang, M. H.; Nguyen, D. N.; Choi, D. H. *Adv. Nat. Sci. Nanosci. Nanotechnol.* **2011**, *2*, 035002/1–035002/7.
26. Seguy, I.; Jolinat, P.; Destruel, P.; Farenc, J.; Mamy, R.; Bock, H.; Ip, J.; Nguyen, T. P. *J. Appl. Phys.* **2001**, *89*, 5442–5448.
27. Vollbrecht, J.; Kasdorf, O.; Quiring, V.; Suche, H.; Bock, H.; Kitzerow, H.-S. *Appl. Phys. Lett.* **2013**, *103*, 043303/1–043303/4.
28. *Chemistry of Discotic Liquid Crystals: From Monomers to Polymers*; Kumar, S., Ed.; CRC Press: Boca Raton, FL, 2010.
29. Mejia, A. F.; Chang, Y.-W.; Ng, R.; Shuai, M.; Mannan, M. S.; Cheng, Z. *Phys. Rev. E Stat., Nonlinear, Soft Matter Phys.* **2012**, *85*, 061708/1–061708/12.
30. Foster, E. J.; Jones, R. B.; Lavigueur, C.; Williams, V. E. *J. Am. Chem. Soc.* **2006**, *128*, 8569–8574.
31. Lavigueur, C.; Foster, E. J.; Williams, V. E. *Liq. Cryst.* **2007**, *34*, 833–840.
32. Voisin, E.; Johan Foster, E.; Rakotomalala, M.; Williams, V. E. *Chem. Mater.* **2009**, *21*, 3251–3261.
33. Paquette, J. A.; Yardley, C. J.; Psutka, K. M.; Cochran, M. A.; Calderon, O.; Williams, V. E.; Maly, K. E. *Chem. Commun.* **2012**, 8210–8212.
34. Ibarra-Avalos, N.; Gil-Villegas, A.; Richa, A. M. *Mol. Simul.* **2007**, *33*, 505–515.
35. Fartaria, R. P. S.; Javid, N.; Sefcik, J.; Sweatman, M. B. *J. Colloid Interface Sci.* **2012**, *377*, 94–104.
36. Marechal, M.; Cuetos, A.; Martinez-Haya, B.; Dijkstra, M. *J. Chem. Phys.* **2011**, *134*, 094501/1–094501/12.
37. Martinez-Haya, B.; Cuetos, A. *J. Chem. Phys.* **2009**, *131*, 074901/1–074901/8.
38. Cuetos, A.; Martinez-Haya, B. *J. Chem. Phys.* **2008**, *129*, 214706/1–214706/7.
39. Del Rio, E. M.; Galindo, A.; De Miguel, E. *Phys. Rev. E Stat., Nonlinear, Soft Matter Phys.* **2005**, *72*, 051707/1–051707/12.
40. Chen, S.; Raad, F. S.; Ahmida, M.; Kaafarani, B. R.; Eichhorn, S. H. *Org. Lett.* **2013**, *15*, 558–561.
41. McGrath, K. K.; Jang, K.; Robins, K. A.; Lee, D.-C. *Chem.—Eur. J.* **2009**, *15*, 4070–4077.
42. Hu, J.; Zhang, D.; Jin, S.; Cheng, S. Z. D.; Harris, F. W. *Chem. Mater.* **2004**, *16*, 4912–4915.
43. Leng, S.; Wex, B.; Chan, L. H.; Graham, M. J.; Jin, S.; Jing, A. J.; Jeong, K.-U.; Van Horn, R. M.; Sun, B.; Zhu, M.; Kaafarani, B. R.; Cheng, S. Z. D. *J. Phys. Chem. B* **2009**, *113*, 5403–5411.
44. Leng, S.; Chan, L. H.; Jing, J.; Hu, J.; Moustafa, R. M.; Van Horn, R. M.; Graham, M. J.; Sun, B.; Zhu, M.; Jeong, K.-U.; Kaafarani, B. R.; Zhang, W.; Harris, F. W.; Cheng, S. Z. D. *Soft Matter* **2010**, *6*, 100–112.
45. Kaafarani, B. R.; Lucas, L. A.; Wex, B.; Jabbour, G. E. *Tetrahedron Lett.* **2007**, *48*, 5995–5998.
46. Lucas, L. A.; De Longchamp, D. M.; Richter, L. J.; Kline, R. J.; Fischer, D. A.; Kaafarani, B. R.; Jabbour, G. E. *Chem. Mater.* **2008**, *20*, 5743–5749.
47. Moustafa, R. M.; Degheili, J. A.; Patra, D.; Kaafarani, B. R. *J. Phys. Chem. A* **2009**, *113*, 1235–1243.
48. Hu, J.; Zhang, D.; Harris, F. W. *J. Org. Chem.* **2005**, *70*, 707–708.
49. Braach-Maksvytis, V.; Raguse, B. *J. Am. Chem. Soc.* **2000**, *122*, 9544–9545.
50. El-Ballouli, A. O.; Khnayzer, R. S.; Khalife, J. C.; Fonari, A.; Hallal, K. H.; Timofeeva, T. V.; Patra, D.; Castellano, F. N.; Wex, B.; Kaafarani, B. R. *J. Photochem. Photobiol., A* **2013**, *272*, 49–57.
51. Kaafarani, B. R.; El-Ballouli, A. a. O.; Trattnig, R.; Fonari, A.; Sax, S.; Wex, B.; Risko, C.; Khnayzer, R. S.; Barlow, S.; Patra, D.; Timofeeva, T. V.; List, E. J. W.; Brédas, J.-L.; Marder, S. R. *J. Mater. Chem. C* **2013**, *1*, 1638–1650.
52. Lee, H.; Harvey, R. G. *J. Org. Chem.* **1986**, *51*, 2847–2848.
53. Connor, D. M.; Allen, S. D.; Collard, D. M.; Liotta, C. L.; Schiraldi, D. A. *J. Org. Chem.* **1999**, *64*, 6888–6890.
54. Suhan, N. D.; Loeb, S. J.; Eichhorn, S. H. *J. Am. Chem. Soc.* **2013**, *135*, 400–408.
55. Donnio, B.; Heinrich, B.; Allouchi, H.; Kain, J.; Diele, S.; Guillon, D.; Bruce, D. W. *J. Am. Chem. Soc.* **2004**, *126*, 15258–15268.
56. Demenev, A.; Eichhorn, S. H.; Taerum, T.; Perepichka, D. F.; Patwardhan, S.; Grozema, F. C.; Siebbeles, L. D. A.; Klenkler, R. *Chem. Mater.* **2010**, *22*, 1420–1428.
57. Wu, J.; Watson, M. D.; Müllen, K. *Angew. Chem., Int. Ed.* **2003**, *42*, 5329–5333.
58. Morale, F.; Date, R. W.; Guillon, D.; Bruce, D. W.; Finn, R. L.; Wilson, C.; Blake, A. J.; Schröder, M.; Donnio, B. *Chem.—Eur. J.* **2003**, *9*, 2484–2501.
59. Anthony, J. *Chem. Rev.* **2006**, *106*, 5028–5048.
60. Kestemont, G.; de Halleux, V.; Lehmann, M.; Ivanov, D. A.; Watson, M.; Geerts, Y. H. *Chem. Commun.* **2001**, 2074–2075.